CORONAL MAGNETIC FIELDS PRODUCED BY PHOTOSPHERIC SHEAR

P.A. Sturrock
Center for Space Science and Astrophysics
Stanford University

W-H. Yang
Center for Atmospheric and Space Sciences
Utah State University

CSSA-ASTRO-87-17
October 1987

CORONAL MAGNETIC FIELDS PRODUCED BY PHOTOSPHERIC SHEAR

P.A. Sturrock and W-H. Yang

ABSTRACT

We use the magneto-frictional method for computing force-free fields to examine the evolution of the magnetic field of a line dipole, when there is relative shearing motion between the two polarities. We find that the energy of the sheared field can be arbitrarily large compared with the potential field. We also find that it is possible to fit the magnetic energy, as a function of shear, by a simple functional form.

I. INTRODUCTION

Stressed coronal magnetic fields play a key role in solar activity, providing the energy for solar flares and possibly for related activity such as surges and coronal mass ejections. (See, for instance, Priest 1982.) By "stressed," we mean that the coronal magnetic field is not current-free so that it is in a higher energy state than the corresponding magnetic field with the same normal magnetic field at the photosphere but without coronal currents. It is therefore important to try to understand the way in which such stressed magnetic-field configurations can develop and to estimate the "free energy" in such configurations. The "free energy" is the excess of the magnetic-field energy of

the current-carrying field above that of the corresponding current-free field.

There are several ways in which currents can develop in coronal magnetic-field configurations. One possibility is that a twisted flux tube emerges from below the photosphere. Another possibility is that two or more distinct flux systems are adjacent to each other, so that current sheets develop at the boundaries. The third possibility is that a field initially in a current-free state is stressed by photospheric motion. This is the possibility that we consider in this article.

Unfortunately, we do not yet have systematic data concerning the horizontal velocity fields of solar active regions. The new development of "correlation tracking," that has been demonstrated on a short span of data acquired during the Spacelab II mission (Simon et al. 1988), holds out the promise that such data can be acquired by spacecraft in the future. Such data would be most valuable in furthering our understanding of solar activity.

Nevertheless, there is circumstantial information indicating that horizontal velocity fields do play a significant role in stressing coronal magnetic fields. For instance, the occurrence of homologous sequences of flares indicates that, once a flare has occurred and returned the magnetic field to something approximating a current-free state, the field is again stressed so that another flare can occur, and so on. (See, for instance, Svestka 1976.) The

similarity of flares in such sequences argues against attributing the re-stressing of the field to the eruption of new magnetic flux. It seems more likely that the progressive re-stressing is to be attributed to a steady photospheric horizontal velocity field.

It is well known that large solar flares are typically of the "two-ribbon" type and occur in active regions with pronounced filaments (Svestka 1976). Filaments occur in the vicinity of magnetic reversal lines. The structure of filaments and vector magnetograms both indicate that the field is highly sheared at the reversal line in such cases.

For these reasons, we are particularly interested in the coronal magnetic-field configurations that develop above photospheric regions containing a linear magnetic dipole, when there is a shear-like displacement on opposite sides of the dipole. In examining this problem, we assume that the density and pressure of the coronal gas are sufficiently small that the magnetic field is unaffected by gravitational and pressure forces. However, the electrical conductivity of the coronal gas will still be sufficiently high that the magnetic field is "frozen" into the coronal plasma. In such situations, the magnetic field will be force-free, and we are therefore faced with the problem of calculating force-free magnetic-field configurations (Priest 1982).

A procedure for calculating such configurations was developed some time ago by Sturrock and Woodbury (1967), and one example of such a configuration was calculated at that

time. We present in this article a series of calculations which we have made using an improved computational procedure described in a recent article (Yang, Sturrock and Antiochos 1986).

The quantity of greatest interest is the total magnetic energy in such a sheared magnetic-field configuration. This will of course be a function of the magnitude of the shear. We find that the results of our detailed calculations may be fit by a simple formula that may prove useful in estimating the amount of energy in similar configurations.

II. FORCE-FREE-FIELD CALCULATIONS

In a recent article, Yang, Sturrock and Antiochos (1986) have proposed a new method for computing force-free magnetic-field configurations that they term the "magneto-frictional method." This procedure has been applied to the present problem. The magnetic field is expressed in terms of Clebsch variables

$$\vec{B} = \nabla\alpha \times \nabla\beta \tag{2.1}$$

where α and β are assumed to be of the form

$$\alpha = \alpha(x,y), \quad \beta = z - \gamma(x,y). \tag{2.2}$$

We see that

$$B_x = \frac{\partial\alpha}{\partial y}, \; B_y = -\frac{\partial\alpha}{\partial x}, \; B_z = -\frac{\partial\alpha}{\partial x}\frac{\partial\gamma}{\partial y} + \frac{\partial\alpha}{\partial y}\frac{\partial\gamma}{\partial x}. \tag{2.3}$$

Since α and β are each constant along a field line, it is clear that the function $\gamma(x,y)$ shows how each field line is displaced in the z direction.

In this model, the plane $y = 0$ is taken to be the photosphere, and the z axis is the axis of the line dipole. Hence the normal component of the photospheric magnetic field is $B_y(x,0)$.

We have adopted

$$\alpha(x,0) = \exp(-x^2/x_0^2) \tag{2.4}$$

so that

$$B_y(x,0) = \frac{2x}{x_0^2} \exp(-x^2/x_0^2) . \tag{2.5}$$

We have also assumed that the region of the photosphere within the band $|x| < x_1$ is subject to shearing motion parallel to the z axis but that there is no shearing motion outside that band. Our specific assumption is that

$$\gamma(x,0) = \begin{cases} Z \sin\left(\frac{\pi x}{x_1}\right) \left| \sin\left(\frac{\pi x}{x_1}\right)\right| , & |x| < x_1 \\ 0 , & |x| > x_1 \end{cases} . \tag{2.6}$$

Hence x_o is a measure of the width of the magnetic dipole, and Z is a measure of the relative shear of the two parts of the dipole.

In carrying out calculations used in the magneto-frictional method, it is necessary to introduce a fictitious outer boundary within which the entire magnetic field is contained. In our calculations, we adopted a mesh such that $x_o = x_1 = 4$. The outer boundary is formed by the lines $x = \pm 20$ and $y = 40$. We imposed the condition $\alpha = 0$ on this boundary, which is equivalent to assuming that the boundary is "superconducting."

Some of the results of our calculations are shown in Figure 1. Figure 1a shows the contours α = constant in the x-y plane for the current-free case ($Z = 0$). Figure 1b shows the corresponding contours for the case $Z = 10$. These contours are the projections of field lines onto the x-y plane, and therefore give the "end-on" view of field lines. Figure 1c gives the same contours in the y-z plane, showing the "side view" of the field lines. Figure 1d shows the contours in the x-z plane, representing the "top view" of the field lines.

We note that, as found earlier by Sturrock and Woodbury (1967), the effect of the shear displacement is to "inflate" the magnetic field configuration, since the development of the B_z component has the same effect as gas pressure. In this context, it is interesting to note that B_z = constant along each field line (see Appendix A).

In Figure 2, we give the total energy of the magnetic field as a function of the shearing parameter Z. There is an important difference between this curve and the

corresponding curve for the case of cylindrical symmetry given in Yang, Sturrock and Antiochos (1986). In the case of cylindrical symmetry, the total energy tends asymptotically to the (finite) energy of the open field. Such behavior is not possible in the present geometry, since the energy of the corresponding open-field configuration is infinite.

Another important difference between the present model and both the earlier model of Sturrock and Woodbury (1967) and the cylindrical case just referred to, is that there is, in the present model, an outer shell of magnetic flux that does not suffer shearing displacement. These field lines therefore tend to restrain the tendency of the inner flux region to expand into an open configuration. As a result, the outer boundary has a less severe effect on these calculations than in the previous cases.

III. EMPIRICAL MODEL FOR MAGNETIC ENERGY VARIATION

A single numerical calculation yields an exact answer to a single question, but an analytical solution shows how the quantity of interest depends on the parameters characterizing the problem. It would be very convenient to have an understanding of the variation of the total magnetic energy as a function of shear and, for this reason, we have attempted to find a simple functional form that approximates the form of the curve shown in Figure 2.

If S is a normalized measure of the shear, such as Z/W, where W is a measure of the width of the bipolar

region, we expect that the total magnetic energy U can be expressed as

$$U = U_0 \, F(S), \tag{3.1}$$

where U_0 is the total energy of the current-free field that corresponds to $S = 0$. Hence $F(0) = 1$. It is also clear that F must be an even function of S so that it is expressible as a function of S^2.

We now consider the asymptotic state of the magnetic field for very large values of S. As S tends to infinity, the magnetic field is driven more and more towards an open configuration. For some very large value of S, we expect that the field is substantially open as far as a radius $r = KS$, but remains substantially dipolar in form for $r > KS$. Hence for $r < KS$, $B \propto r^{-1}$, whereas for $r > KS$, $B \propto r^{-2}$.

One may therefore estimate the dominant contribution to the magnetic energy by calculating the energy of the magnetic field as far as $r = KS$:

$$U(S) \propto \int_{r_0}^{KS} \pi r \, dr \, . \, \frac{1}{8\pi} \, \frac{1}{r^2} \tag{3.2}$$

Hence we expect that, for large values of S,

$$U(S) \propto \ln S \tag{3.3}$$

A simple function that has this asymptotic behavior, is an even function of S, and reduces to U_0 for $S = 0$, is

$$U(S) = U_o \, [1 + A \, \ln(1 + BS^2)] \, . \qquad (3.4)$$

In Table 1, we give the calculated values of U for Z in the range 0 to 16. Adopting S = Z/W and W = 4 (so that 2Z is the maximum displacement of any field line, and 2W is a measure of the total width of the field distribution), the values of S are as shown in the table. We have made a least-squares fit to these data and found that the best fit is obtained for A = 0.847, B = 0.862. With these values, the formula (3.4) yields the estimates of U shown in column 4 of Table 1. The same data are shown in Figure 2. We see that the average discrepancy between the estimated and the actual values of the energy is less than 1%. For large values of S, the formula yields values of U less than those that we have computed. For such large values of S, the boundary is beginning to affect the computed magnetic field, and its effect is such that the computed energy will be higher than the real energy. We are exploring methods to reduce the influence of the outer boundary, and it will be interesting to see whether or not the fit of the above functional form to the data improves.

IV. DISCUSSION

We have seen from Section II that relative shearing motion of the two sides of a line dipole leads to "inflation" of the magnetic-field pattern and to a progressive increase in the stored magnetic energy. For

such a model, the magnetic energy can, in principle, become arbitrarily large. Hence the free energy of a stressed magnetic field in an active region may in fact be considerably larger than the energy of the corresponding potential field. In this respect, the linear dipole configuration differs significantly from cylindrically symmetrical models, such as the one considered by Yang, Sturrock and Antiochos (1986).

We have found, in Section III, that a simple model provides a good fit to the results of the force-free-field calculations. We have also examined a similar--but different--model computed some time ago by Woodbury and found that the same formula (equation 3.4) gives a good fit to the data, the mean error being of order 0.1%. We intend to examine other models. If it is found that the same formula is useful for a wide range of models, the problem of computing stored energy as a function of shear would become greatly simplified: it would be sufficient to calculate only the current free field and two stressed configurations.

It is interesting also to note from equation (3.4) that the force opposing the shear varies with Z as follows:

$$F \equiv \left| \frac{dU}{dS} \right| = \frac{2ABU_0 S}{1+BS^2} , \qquad (4.1)$$

so that it varies linearly with Z for small values of Z and inversely with Z for large values of Z. The maximum value of F is $2AU_0$ at $S = B^{-1/2}$. Since the normal

field B_y is being held constant at the "photosphere," the above variation in F must be attributed to a progressive change in the value B_z, the component of field in the direction of shear: B_z first increases and then decreases with Z.

The fact that the magnetic energy, as a function of shear, may be expressed in a simple functional form suggests that it may be possible to find a simple approximate representation of the magnetic field itself.

This work was supported in part by Office of Naval Research Contract N00014-85-K-0111, by NASA Grant NGL 05-020-272, and as part of the Solar-A collaboration under NASA Contract NAS8-37334 with Lockheed Palo Alto Research Laboratories.

APPENDIX

Demonstration that B_z = const. along a field line.

We see from equation (2.3) that B may be expressed as

$$B = \left(\frac{\partial \alpha}{\partial y} , - \frac{\partial \alpha}{\partial x} , B_z \right) . \qquad (A.1)$$

Hence the current density j may be expressed as

$$j = \frac{1}{4\pi} \left(\frac{\partial B_z}{\partial y} , - \frac{\partial B_z}{\partial x} , - \frac{\partial^2 \alpha}{\partial x^2} - \frac{\partial^2 \alpha}{\partial y^2} \right) . \qquad (A.2)$$

The Lorentz force is zero for a force-free field, so the expression for the z-component of this force leads to the relation

$$\frac{\partial B_z}{\partial x}\ \frac{\partial \alpha}{\partial y} - \frac{\partial B_z}{\partial y}\ \frac{\partial \alpha}{\partial x} = 0 \ . \qquad (A.3)$$

This shows that the projections of ∇B_z and $\nabla\alpha$ in the x-y plane are parallel. However, B_z and α are independent of z, so ∇B_z is parallel to $\nabla\alpha$. We see from equation (2.1) that $B.\nabla\alpha = 0$. Hence $B.\nabla B_z = 0$, showing that B_z = const. along a field line.

TABLE 1

Comparison of Computed Energy (U) and Best Fit (U')

S	U	U'
0.00	1.012	1.012
0.25	1.062	1.057
0.50	1.189	1.178
0.75	1.354	1.348
1.00	1.535	1.541
1.25	1.900	1.929
1.75	2.075	2.111
2.00	2.243	2.281
2.25	2.404	2.440
2.50	2.558	2.589
2.75	2.706	2.728
3.00	2.847	2.858
3.25	2.983	2.979
3.50	3.115	3.094
3.75	3.242	3.201
4.00	3.366	3.303

REFERENCES

Priest, E.R. 1982, Solar Magnetohydrodynamics (Dordrecht-Holland: Reidel).

Simon, G.W., et al. 1988, Ap. J. (in press).

Sturrock, P.A., and Woodbury, E.T. 1967, in Plasma Astrophysics, ed. P.A. Sturrock (New York: Academic Press), p. 155.

Svestka, Z. 1976, Solar Flares (Dordrecht-Holland: Reidel).

Yang, W.H., Sturrock, P.A., and Antiochos, S.K. 1986, Ap. J., 309, 383.

Figure Captions

Fig. 1 shows various views of the field lines, labeled by the value of α: (a) projections of field lines on the x-y plane, giving the "end-on" view, for the current-free case $Z = 0$; (b) the same as (a), but for the stressed case $Z = 10$; (c) projections on the y-z plane, giving the "side-on" view, for the case $Z = 10$; and (d) projections on the x-z plane, giving the "top" view, for the case $Z = 10$.

Fig. 2. Comparison of the energy of the computed force-free field (shown as dots) with the energy of the best fit of the form given by eq. (3.4) (shown as solid line).

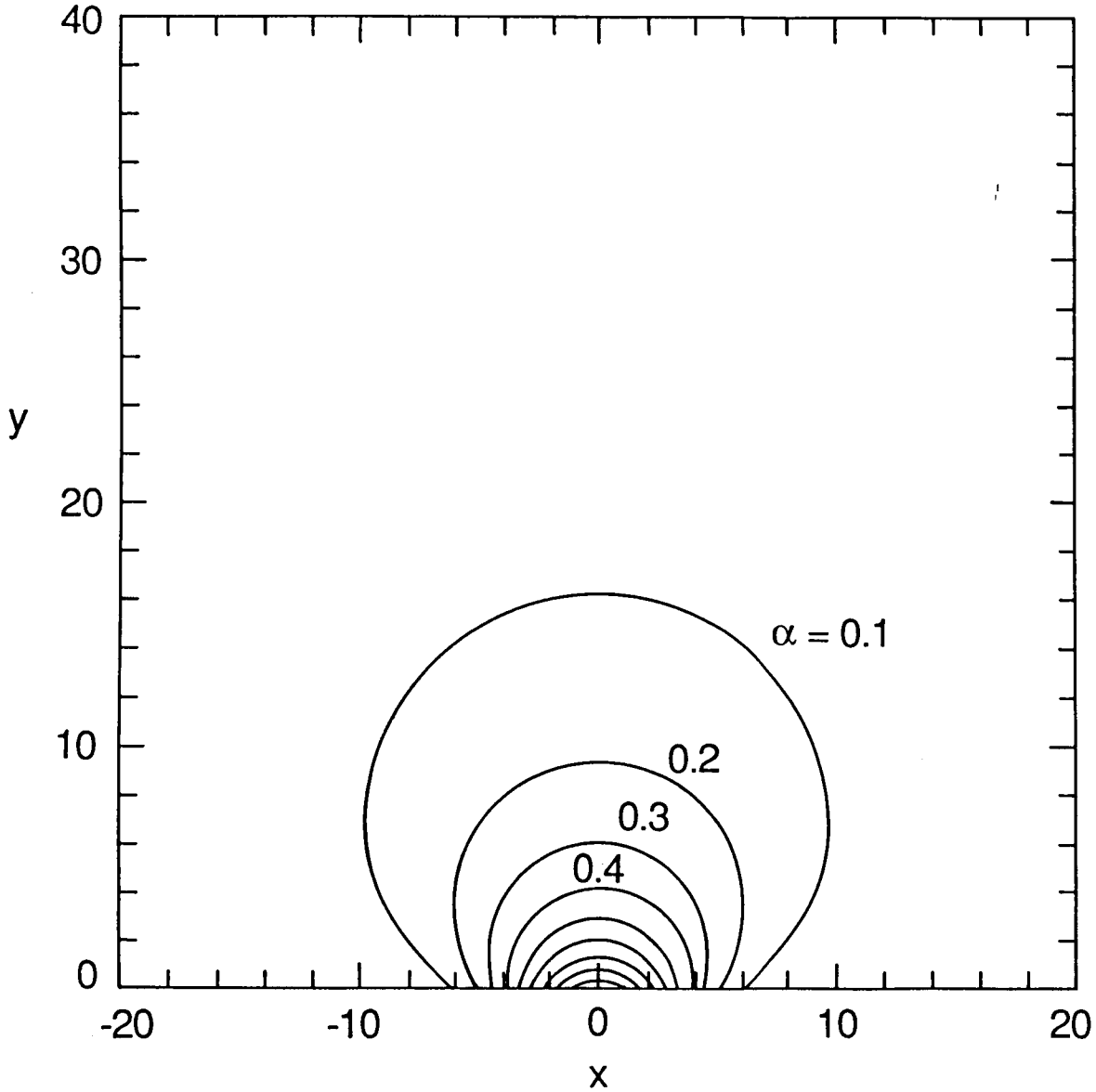

Fig. 1a

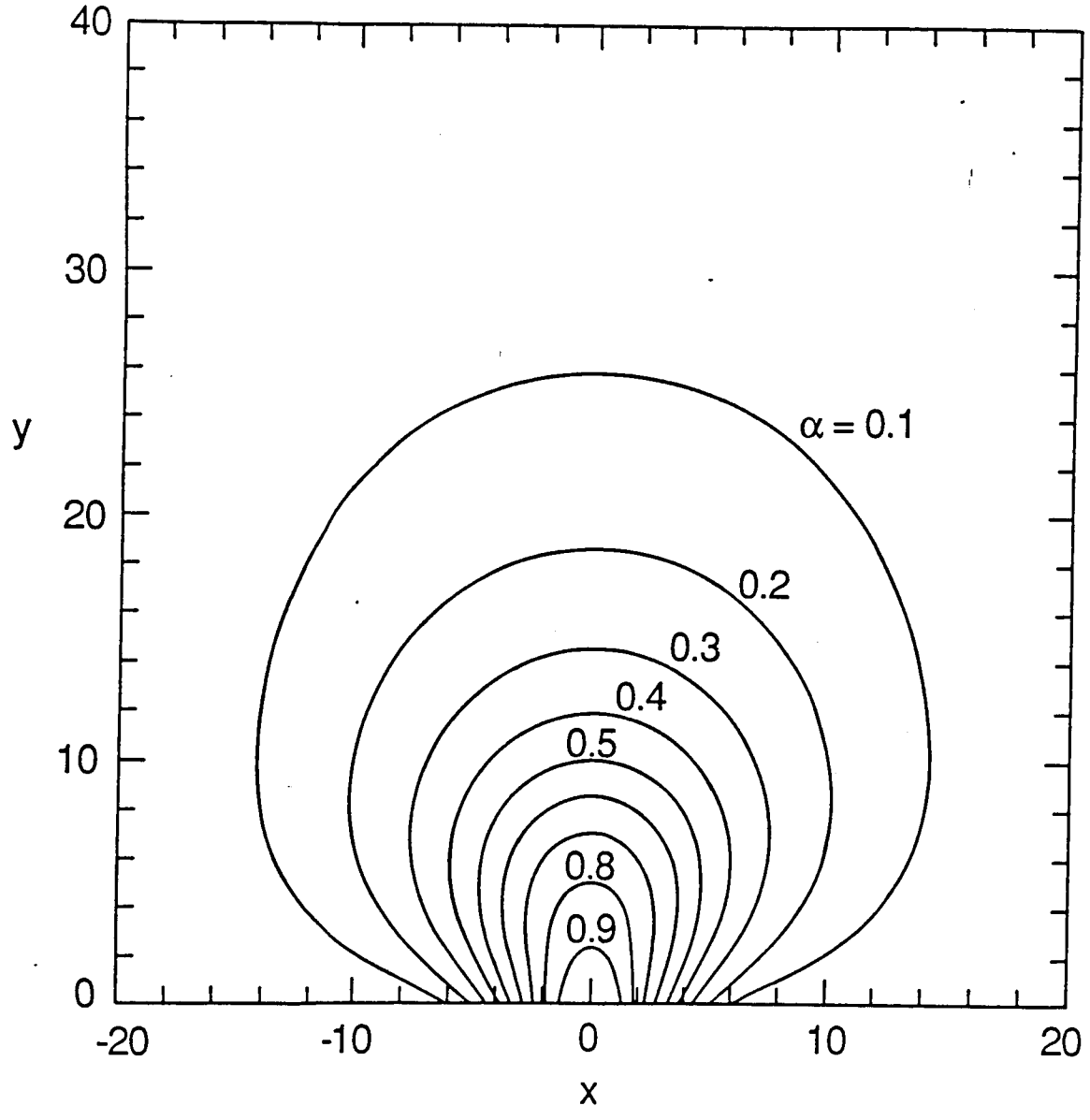

Fig. 1b

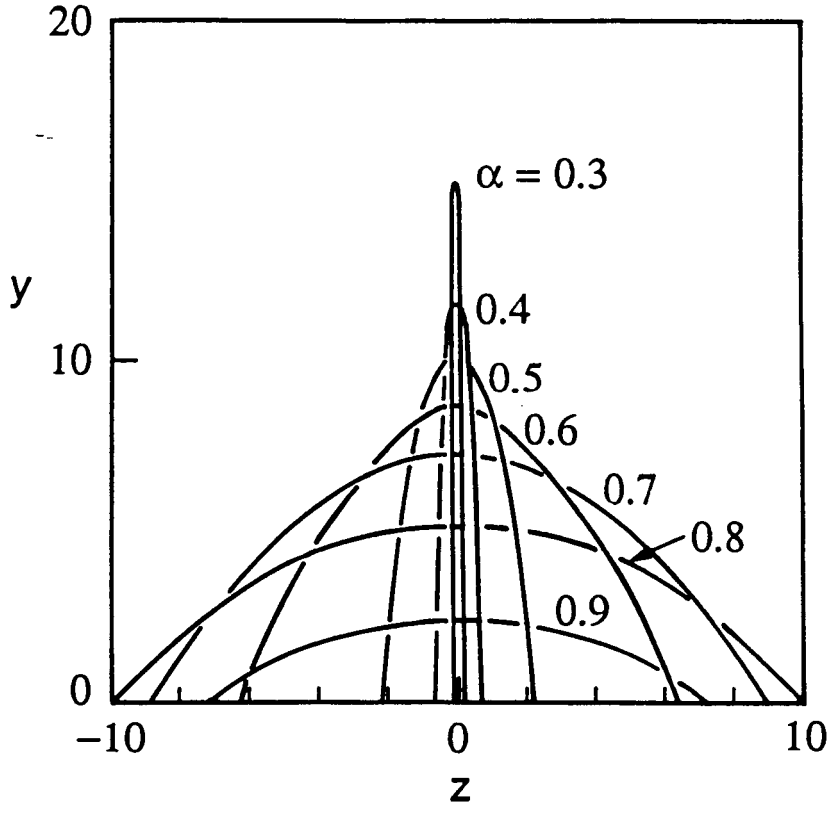

Fig. 1c

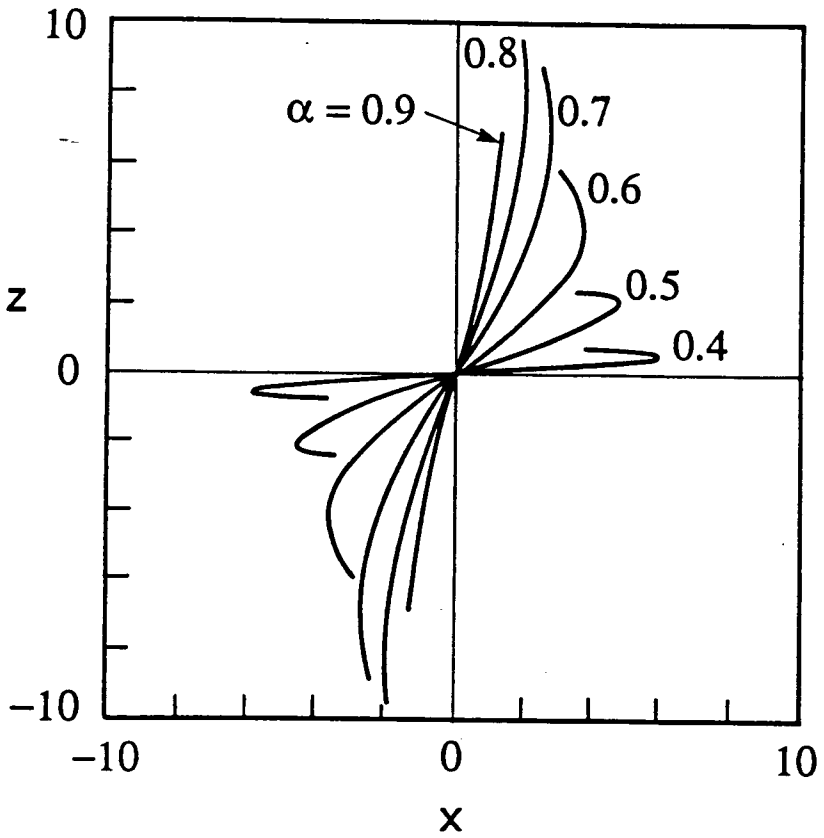

Fig. 1d

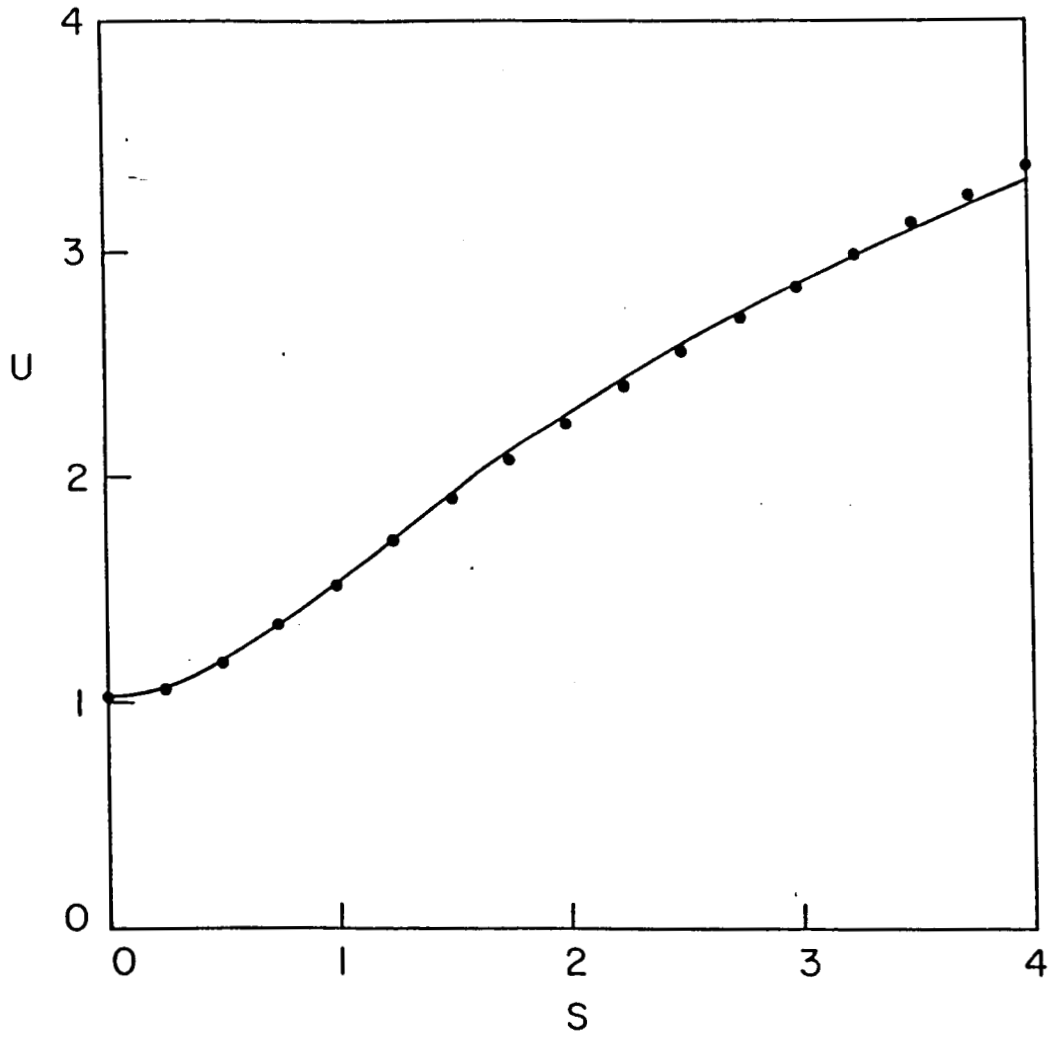

Fig. 2

POSTAL ADDRESS PAGE

PETER A. STURROCK: Center for Space Science and Astrophysics, Stanford University, Stanford, CA 94305

WEI-HONG YANG: Center for Atmospheric and Space Sciences, Utah State University, Logan, UT 84322-4405